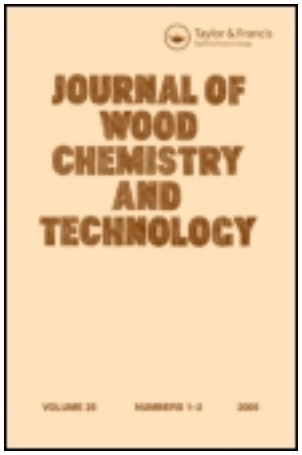

Journal of Wood Chemistry and Technology

Publication details, including instructions for authors and subscription information:
http://www.tandfonline.com/loi/lwct20

Lignin Structural Changes During Liquefaction in Acidified Ethylene Glycol

Edita Jasiukaitytė-Grojzdek [a b], Matjaž Kunaver [a b] & Claudia Crestini [c]

[a] National Institute of Chemistry, Ljubljana, Slovenia

[b] Center of Excellence for Polymer Materials and Technologies, Ljubljana, Slovenia

[c] Tor Vergata University, Rome, Italy

Version of record first published: 11 Jul 2012

To cite this article: Edita Jasiukaitytė-Grojzdek, Matjaž Kunaver & Claudia Crestini (2012): Lignin Structural Changes During Liquefaction in Acidified Ethylene Glycol, Journal of Wood Chemistry and Technology, 32:4, 342-360

To link to this article: http://dx.doi.org/10.1080/02773813.2012.698690

Journal of Wood Chemistry and Technology, 32:342–360, 2012

ISSN: 0277-3813 print / 1532-2319 online
DOI: 10.1080/02773813.2012.698690

Lignin Structural Changes During Liquefaction in Acidified Ethylene Glycol

EDITA JASIUKAITYTĖ-GROJZDEK,[1,2] MATJAŽ KUNAVER,[1,2] AND CLAUDIA CRESTINI[3]

[1]National Institute of Chemistry, Ljubljana, Slovenia
[2]Center of Excellence for Polymer Materials and Technologies, Ljubljana, Slovenia
[3]Tor Vergata University, Rome, Italy

Abstract: *Beech (*Fagus Sylvatica*) milled-wood lignin was used as a model substrate in a study of lignin-catalyzed liquefaction in the presence of* p*-toluene sulfonic acid monohydrate (PTSA) or sulphuric acid as the catalysts. The structural changes that lignin undergoes during the treatment were studied by NMR spectroscopy, FTIR, size-exclusion chromatography, and high-performance liquid chromatography. For the sulphuric acid-catalyzed liquefaction, it was shown that the greater hydronium ion concentration in the reaction mixture induced formation of more condensed structures compared to the ones obtained after PTSA-catalyzed liquefaction. In addition, lignin during the PTSA-catalyzed liquefaction suffered degradation and was functionalized by the ethylene glycol. Gradual introduction of the ethylene glycol moieties into the lignin structure formed a condensed lignin-based polymeric material with predominant aromatic hydroxyl groups. HPLC and NMR analysis of the liquefied lignin with low-molecular mass fraction confirmed the presence of lignin monomers and further conversion of initially identified products into the aliphatic, aromatic (syringyl- and guaiacyl-based) esters and acids.*

Keywords Lignin, liquefaction, ^{31}P NMR, ^{13}C NMR, size-exclusion chromatography, high-performance liquid chromatography

Introduction

One of the major reasons behind the increasing demand to reduce the reliance on fossil fuels is the fact that they are expected to run out in the future. Among renewable resources such as biomass, hydropower, solar, geothermal, wave, tidal, and wind resources, biomass is the only organic resource. Accordingly, biomass is widely applicable and can be converted to useful fuels and chemicals, such as those produced by oil refineries, to maintain a high degree of industrialization.

One of the major lignocellulosic biomass transformation pathways commonly used is thermochemical conversion (liquefaction) with the use of different liquefying agents

The authors acknowledge financial support from the Ministry of Higher Education, Science and Technology of the Republic of Slovenia and Slovenian Research Agency (programme P2-0145).

Address correspondence to Edita Jasiukaitytė-Grojzdek, National Institute of Chemistry, Hajdrihova 19, Ljubljana 1000, Slovania. E-mail: ejasiukaityte@yahoo.com

and catalysts. Here, solvolysis and depolymerization take place simultaneously, forming a final product that is rich in hydroxyl group functionality. The liquefaction process is well known and has been the subject of several studies.[1–4] A lignocellulosic biomass liquefaction reaction, performed under acidic conditions with liquefying reagents, such as phenol or polyhydric alcohols, produces a new potential feedstock for the synthesis of bio-based materials.[5–7] Liquefied lignocellulosic biomass maintains multiple hydroxyl groups, which are used as reactive sites in the preparation of polyesters, polyurethanes, and fuels.[8–10] The lignocellulose liquefaction mechanism is complex and not fully understood. There have been few attempts made to thoroughly describe the reaction pathway using model compounds. A mechanism of cellulose degradation in acidified ethylene glycol was proposed by Yamada and Ono.[11] Lin et al. tried to clarify the mechanism of the cellulose reaction with phenol under acid-catalyzed conditions using cellobiose as a model compound.[12] Cellulose powder, steamed lignin, and the mixtures of these two components have been used by Kobayashi et al.[4] to study the reaction process during liquefaction with polyhydric alcohol with an emphasis on residue formation analysis. It was suggested that the condensation reaction was a result of mutual reactions between depolymerized cellulose and aromatic derivatives of lignin. The occurrence of the intensive condensation reaction during the wood liquefaction between the solubilized products was reported by Kurimoto et al.[5] The cited authors observed a significant retardant effect on the condensation when the liquefaction of different wood species was performed in a glycerol-containing polyethylene glycol system. According to their study, there are obviously distinct interactions between the lignin fragments and the liquefying agent that inhibits the so-called re-condensation.

Thus far, liquefaction of lignin has been studied on the basis of model substances, such as guaiacylglycerol-β-guaiacyl ether.[13,14] However, it is difficult to predict the reactions of a three-dimensional biopolymer composed of three different monomers which are inter-connected with several types of bonds during liquefaction using a monomeric lignin model compound, even though it represents the most dominant type of bonding in lignin structure. Lignin's behavior during wood liquefaction in a glycerol-containing diethylene glycol system has been studied by Jasiukaitytė et al.[15] With the use of *p*-toluene sulfonic acid monohydrate as a catalyst, they successfully increased the wood content in a liquefaction mixture and reduced the self-polymerization reactions of lignin that consequently prevented the formation of undesirable insoluble residue over the prolonged wood liquefaction. According to the cited authors, the solubility of the final product increased because the liquefying agent was incorporating into the lignin structure.

The possible novel lignin modification reactions that occur under the described liquefaction conditions could be an avenue for new polymeric lignin materials whose glass transition temperature could be controlled and lowered due to the free volume introduced by the ethylene glycol chains or eventually by any analogous glycol. This could be an area for future investigation with technical (kraft) lignins that could offer potential benefits.

The lack of information on lignin liquefaction motivates our comprehensive study of a pure lignin liquefaction pathway by identification and structural characterization of the lignin-derived products. The use of a specifically isolated milled-wood lignin (MWL), representative of the original lignin in lignocellulose, is particularly important for the elucidation of lignin's influence on the undesirable condensation reactions and to facilitate the discovery of potential mechanisms that increase the solubility of the obtained lignin derivatives.

In this study, the liquefaction of beech MWL was carried out in the presence of ethylene glycol under the catalysis of sulphuric acid or *p*-toluene sulfonic acid monohydrate catalysis. Two different catalysts were used in order to determine the influence of hydronium ion

concentration to the intensity of lignin self-polymerization. Ethylene glycol as a polyhydric alcohol with the simplest structure was chosen for its easy interpretation of the obtained lignin derivatives.

The precipitation of the liquefied lignin samples into the acidified water enabled the separation of high-molecular mass material (LBP) from low-molecular mass glycol fraction (LGS), and both (LBP and LGS) were used to study the lignin liquefaction. The lignin reactions during the liquefaction were studied by evaluating aromatic and aliphatic hydroxyl group contents over time. In addition, the amount of incorporated aliphatic ethylene glycol chains into the lignin macromolecule was quantified by monitoring the change of molar masses and by identification of low-molecular mass compounds obtained after the degradation of lignin structure.

Experimental

Materials

Milled-wood lignin was isolated from beech (*Fagus sylvatica L.*) according to the previously described procedures.[16–18] Ethylene glycol (EG, Merck), *p*-toluene sulfonic acid monohydrate (PTSA, Acros Organics), 97% sulphuric acid (H_2SO_4, Merck), Tetrahydrofuran (THF, Merck), Methanol (Merck), Acetic acid (Merck), *N,N*-dimethylacetamide for HPLC (DMA, Fluka), lithium bromide (LiBr, Aldrich), *N*-hydroxynaphthalimide (Acros Organics), chromium (III) acetylacetanoate (Acros Organics), 2-chloro-1,3,2-dioxaphospholane (Fluka), 2-chloro-4,4,5,5-tetramethyl-1,3,2-dioxaphospholane (Aldrich), 1,3,5-trioxane (Aldrich), deuterated chloroform ($CDCl_3$-*d*, Merck), and deuterated dimethylsulfoxide (DMSO-d_6, Merck) were of reagent grade and were used without further purification.

Lignin Liquefaction

Beech milled-wood lignin was liquefied with EG in the ratio of 1:5. The liquefaction was carried out in a rounded flask (two necks), equipped with a stirrer (IKA Labortechnik) and condenser. To catalyze the reaction 3% w/w (based on the EG) of the catalyst (PTSA or H_2SO_4) was added to the reaction mixture. Ethylene glycol was chosen as a polyhydric alcohol with the shortest aliphatic chain in order to simplify the elucidation of the lignin liquefaction pathway. The liquefaction mixture was heated for 4 h at 150°C in a silicon oil bath while being constantly stirred at 400 rpm. Samples from the reaction mixture were taken at different time intervals and immediately cooled in an ice-bath to quench the reaction.

Sample Preparation

Liquefied lignin samples were precipitated from the excess of acidified distilled water. The precipitate was collected by centrifugation for 10 min at 4500 rpm, freeze-dried, and designated as a "lignin-based polymer" (LBP). The supernatant was collected, neutralized with 0.1 N NaOH solution, and concentrated under reduced pressure at 35 – 40°C. The product was then added drop-wise into 96% ethanol. The obtained white precipitate was filtered using a filter paper and was identified as sodium chloride with infrared spectroscopy. The ethanol was removed by rotary evaporation and the sample was assigned as a "lignin-glycol sample" (LGS).

The amount of the LBP formed during the lignin liquefaction was defined as follows:

$$LBP\,(\%) = (W^t_{LBP}/\mathrm{W}^{\mathrm{t}}_0) \times 100 \quad (1)$$

where W^t_0 is the weight of liquefied lignin sample that was precipitated into acidified water and W^t_{LBP} is the weight of LBP.

Acetylation

The precipitated LBP samples were acetylated with pyridine/acetic anhydride (2:1) v/v mixture for 8 h at 50°C. After 8 h, the pH of the solutions was adjusted to ∼3.0 with 0.1 N HCl and left at room temperature for 12 h with continuous stirring. The obtained suspensions were centrifuged for 10 min at 4500 rpm, repeatedly washed with distilled water (5×10 cm^3), and freeze-dried.

FTIR Spectroscopic Analysis

LBP samples were analyzed using a Perkin-Elmer Spectrum 100 FTIR spectrophotometer. The transmittance measurements were conducted using the UATR (Universal Attenuated Total Reflectance) sampling method in the range from 4000 cm^{-1} to 800 cm^{-1}.

NMR Spectroscopy

Qualitative ^{13}C NMR, DEPT (distortionless enhancement by polarization transfer) spectra were recorded using a Unity Inova 300 Varian NMR spectrometer operating at 75 MHz. The measurements were conducted in DMSO-d_6 at 25°C and tetramethylsilane (TMS) was used as an internal standard. A relaxation delay of 2 s was used between the scans. The free induction decay (FID) was multiplied by an exponential factor corresponding to the 4 Hz line broadening prior to performing a Fourier transformation. For each spectrum, typically about 13 500 scans were accumulated.

The quantitative NMR spectra of the LBP samples were recorded as reported elsewhere.[19–21] Quantitative ^{13}C NMR spectra of acetylated LBP samples were recorded with a Bruker 300 MHz spectrometer equipped with a Quad probe dedicated to ^{31}P, ^{13}C, ^{19}F, and ^{1}H acquisition at 308 K using an inverse gated decoupling pulse sequence. A sweep width of 10,000 Hz was observed, and spectra were accumulated with time delay of 12 s between pulses. A pulse width causing 90° flip angle was used. The chemical shifts were referred to the internal standard signal at 93.4 ppm. Line broadening of 4 Hz was applied to FIDs before Fourier transform. For each spectrum, typically about 12,000 scans were accumulated.

The quantitative ^{13}C NMR data reported in this work is a result of a single experiment, while the maximum standard error was calculated for each analysis separately and made approximately 10% of the estimated value. The quantitative ^{31}P NMR data reported in this work are averages of three experiments. The maximum standard deviation of our results was 2×10^{-2} mmol/g, while the maximum standard error was 1×10^{-2} mmol/g.

Size-exclusion Chromatography (SEC)

SEC of lignin-based polymer and lignin-glycol samples was performed on a size-exclusion chromatographic system (HP — AGILENT system) equipped with a UV detector set at

280 nm. Analyses were carried out at ambient temperature using THF and DMA with 0.01 M LiBr as eluents at a flow rate of 1 cm^3/min and 0.7 cm^3/min, respectively. Aliquots (100 μL) of each lignin-based polymer samples (LBP), dissolved in THF (1.5 mg/cm^3), and lignin-glycol samples (LGS), dissolved in DMA with 0.01 M LiBr, were injected into PLgel 3 μm MIXED E 7.5 $\times$ 300 mm and Polar Gel L 8 μm 7.5 $\times$ 300 mm, respectively. The columns specifications allow separation of molecular masses up to 3.0 $\times$ 10^4 g/mol. The SEC system was calibrated with polystyrene standards. The chromatographic data were processed with PSS (Polymer Standards Service) WinGPC Unity software.

High-performance Liquid Chromatography (HPLC)

The detection of lignin phenols was carried out on a Perkin Elmer HPLC system consisting of a binary pump (Series 200 LC) and a diode array detector (L-235) set at 280 nm. Methanol-water (25:75, v/v) with 1% (v/v) addition of acetic acid was used as a mobile phase at a flow rate of 1 cm^3/min at ambient temperature. Aliquots (10 μL) of each glycol sample (LGS) were injected into a stainless-steel column (200 $\times$ 4.6 mm) packed with ODS Hypersil (5 μm). All chemicals used as standards (phenolic acids, coniferyl alcohol, sinapyl alcohol, vanillin, syringaldehyde, furfural, hydroxymethyl furfural, glycerol guaiacol ether, dimethoxyphenol) were purchased from Aldrich. The chromatographic data were processed with PSS (Polymer Standards Service) WinGPC Unity software.

Results and Discussion

Lignin Solvolysis and Formation of Lignin-based Polymer (LBP)

Rapid and complete lignin dissolution was achieved by the applied combination of high temperature, EG concentration, and the amount of catalysts. However, using PTSA as a catalyst, the gradual increase of precipitated high-molecular mass material content with time (Table 1) indicated the presence of interactions between lignin and EG that accordingly led to the formation of condensed polymeric material designated in this study as "lignin-based polymer" (LBP).

The incomplete ($\sim$75%) lignin recovery after 5 min of the PTSA-catalyzed liquefaction can be interpreted in terms of initial lignin degradation followed by the formation of low-molecular mass fragments with increased solubility in acidified polar medium. The increase of isolated LBP content of about 20% by the end of the lignin PTSA-catalyzed liquefaction implies, beside the initial lignin degradation, that lignin self-polymerization

Table 1
The percentage of isolated LBP during the PTSA- and H_2SO_4-catalyzed liquefaction with reaction time

	Recovered lignin sample LBP, %	
Time, min	PTSA $[H^+] = 0.0053$ mol/L	H_2SO_4 $[H^+] = 0.0204$ mol/L
5	74.7	78.9
60	84.7	82.7
120	91.0	76.3
240	94.5	78.0

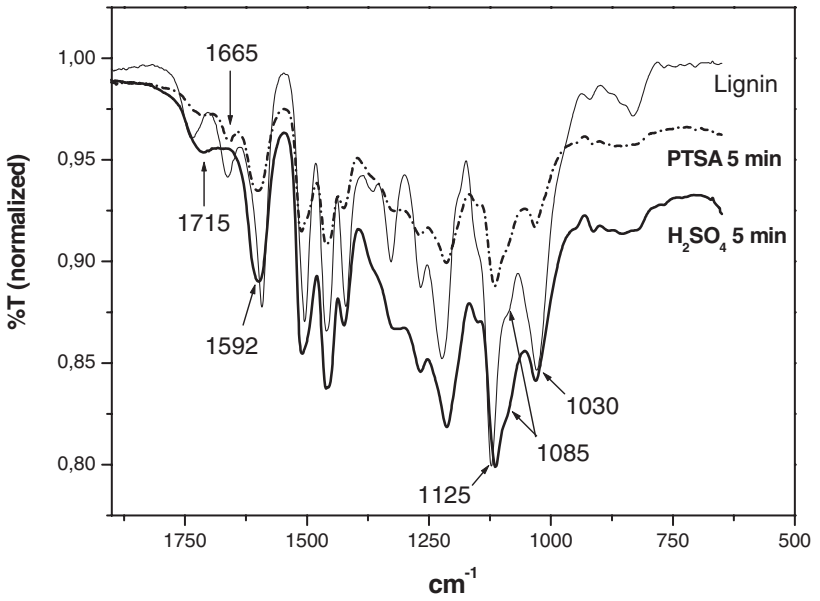

Figure 1. FTIR spectra of lignin and samples taken after 5 min of PTSA- and H_2SO_4-catalyzed lignin liquefaction.

reactions occurred and were followed by condensation with EG, which was used as a liquefying agent. In contrast to the PTSA-catalyzed reaction, the percentage of the isolated LBP did not change significantly for the H_2SO_4 catalysis. Relatively constant amounts of recovered LBP with reaction time show that the lignin functional groups, instead of being functionalized by EG, were involved in lignin self-polymerization (Table 1). The intensive lignin self-polymerization, due to the four times greater hydronium ion concentration in the reaction mixture with H_2SO_4, was considerably faster compared to the PTSA-catalyzed reaction. Furthermore, the greater hydronium ion concentration in the H_2SO_4-catalyzed reaction induced the formation of more condensed lignin-based structures, which were only partially soluble in the common solvents.

FTIR analyses of the LBP samples were performed in order to determine why the LBP structures obtained after the H_2SO_4-catalyzed liquefaction (LBP-H_2SO_4) had limited solubility. The FTIR spectra of the lignin and the samples taken after 5 min of liquefaction are presented in Figure 1. It is evident that the spectrum of LBP obtained after 5 min of PTSA-catalyzed treatment (LBP-PTSA) exhibits all the characteristic absorption bands compared to an untreated lignin sample, though it has a reduced intensity.

In contrast to the LBP-PTSA spectrum, in the LBP-H_2SO_4 spectrum, significant increase in intensity of the absorption band at 1085 cm^{-1} was observed. The intensive absorption band at 1085 cm^{-1} corresponding to C—O deformation in secondary alcohols and aliphatic ethers implies the occurrence of the secondary aliphatic alcohol etherification. Since there were no observable changes in absorption bands at 1030 cm^{-1} (C—O deformations in primary alcohols and C—H in-plane deformation guaiacyl units) and at 1125 cm^{-1} (C—H in-plane deformation of syringyl units), it could be assumed that the secondary aliphatic hydroxyl groups were etherified by EG. Furthermore, every additional primary hydroxyl group obtained after the incorporation of EG molecule or the one within the lignin macromolecule interacted with aromatic ketone group that is suggested by

disappearance of the absorption band at 1665 cm^{-1} (C=O stretching in conjugated *p*-substituted aryl ketones). Analogously, beside the secondary hydroxyl group etherification reactions, they could be oxidized and interact with aromatic hydroxyl group and/or be involved in linkage formation between primary hydroxyl group and aromatic ketone group as suggests the appearance of the large shoulder at 1715 cm^{-1} (C=O stretching in saturated open-chain ketones). In addition, the aromatic ketone group may interact with the aromatic hydroxyl group without EG incorporation, forming an aromatic network that gives rise to the intensive absorption bond at 1592 cm^{-1} (aromatic skeletal vibrations).

From LBP-H_2SO_4 spectra, the assumption could be made that the reason for limited LBP-H_2SO_4 sample solubility is a rapid formation of the rigid aromatic network with obscure EG chain incorporation. The emergence of broad intensive absorption bands in the LBP-H_2SO_4 spectrum is in general characteristic for the highly polymerized structure, which is a result of the intensive lignin self-condensation reactions under acidic treatment.[22]

Therefore, due to the limited solubility of LBP-H_2SO_4 samples in solvents used for NMR and liquid chromatography, only samples obtained after the PTSA-catalyzed reaction were used to investigate lignin structural changes during the acid-catalyzed liquefaction in ethylene glycol.

Quantitative NMR Analysis

In order to evaluate the chemical modifications induced during the lignin liquefaction, detailed characterization of the lignin structure before and after liquefaction was performed using quantitative ^{31}P NMR and ^{13}C NMR. The ^{31}P NMR technique is capable of detecting and quantitatively determining all reactive hydroxy groups, i.e. aliphatic OH, the various forms of phenolic OH and carboxylic acids in lignin. ^{13}C NMR is a powerful technique for obtaining a large amount of lignin structural information, including the presence of aryl ether, condensed and uncondensed aromatic and aliphatic carbons. Using these methodologies, an extensive study of the overall lignin structure before (beech MWL) and after (LBP) the liquefaction reaction was performed.

Quantitative ^{31}P NMR Analysis. Hydroxyl functional groups in isolated beech MWL and LBP samples were submitted to phosphytilation with 2-chloro-1,3,2-dioxaphospholane (**1**), or 2-chloro-4,4,5,5-tetramethyl-1,3,2-dioxaphospholane (**2**), and analyzed by quantitative ^{31}P NMR in the presence of a known amount of N-hydroxynaphthalimide, which was used as the internal standard (IS). Phosphytilation reagents (**1, 2**) react with hydroxyl functional groups to give phosphite products which are resolvable by ^{31}P NMR into separate regions arising from aliphatic hydroxyl, phenolic, and carboxylic acid groups. The integration regions that have been used in this study are listed in Table 2.

The spectra of samples derivatized with 2-chloro-1,3,2-dioxaphospholane enabled the identification of the initial EG attack at C position of the phenyl propane unit in the lignin, as shown in Figure 2.

Incorporation of the EG molecules into the lignin structure consequently eliminated the broad signals in the range of 136.2–134.5 ppm, corresponding to the phosphitylated secondary OH groups in β-O-4 structures in the same manner as was described by Argyropoulos et al.[19] In addition, the absence of any signals in the range of 136.2–134.5 ppm as early as after 5 min of the reaction indicates the extremely high reactivity of the secondary OH with EG under the lignin liquefaction conditions.

Table 2
Integration regions for 2-chloro-1,3,2-dioxaphospholane (**1**) and 2-chloro-4,4′,5,5′-tetramethyl-1,3,2-dioxaphospholane (**2**) treated MWL and LBP samples

Functional group	Integration region (ppm)
N-hydroxynaphthalimide (IS)[1]	138.6–138.0
N-hydroxynaphthalimide (IS)[2]	154.0–153.3
Aliphatic OH[2]	149.3–145.0
Primary aliphatic OH[1] (P—OH)	134.5–132.0
Secondary aliphatic OH[1](S—OH)	136.2–134.5
Syringyl phenolic OH[2] (Sr)	143.0–142.0
Guaiacyl phenolic OH[2] (G)	140.2–138.8
p-Hydroxyphenyl OH[2] (H)	138.8–137.4
COOH[2]	135.5–134.0

Table 3 displays the quantitative information of the distribution of the various OH groups for all the experiments carried out in this study. The spectra of samples derivatized with phosphytilation reagent **2** showed a reduction of the overall aliphatic OH groups from 7.44 to 2.61 mmol/g during a 240 min liquefaction. The sharp decrease of the overall aliphatic OH content from 7.44 to 2.75 mmol/g during a 5 min treatment could be explained by the initial lignin degradation followed by the formation of soluble low-molecular mass lignin derivatives in LGS. In addition to the overall decrease of aliphatic OH content, the *S-OH/P-OH* ratio decrease at the beginning of the treatment indicates the introduction of the EG molecule at Cα position that accordingly yields an appearance of additional *P-OH* from EG (Table 3; Figure 2).

The distribution and quantitative evaluation of phenolic OH and carboxylic acids were obtained from the spectra of samples derivatized with 2-chloro-4,4′,5,5′-tetramethyl-1,3,2-dioxaphospholane.

The overall increase of the phenolic OH content in the LBP with respect to reaction time (from 1.11 to 5.37 mmol/g) may be interpreted in terms of an initial lignin degradation followed by the formation of soluble low-molecular mass lignin derivatives and the cleavage of the β-ethers within the lignin macromolecule.

The more pronounced increase of the syringyl (Sr) phenolic OH (from 0.29 to 2.84 mmol/g) than guaiacyl and *p*-hydroxyphenyl (G + H) phenolic OH (from 0.82 to

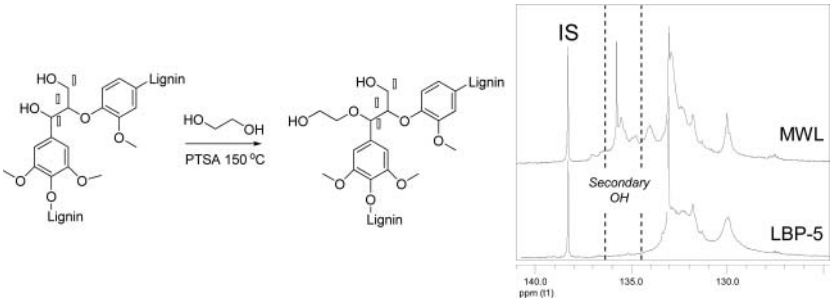

Figure 2. The substitution of secondary hydroxyls in MWL by EG and quantitative ^{31}P NMR spectra of MWL, LBP-5 samples derivatized with 2-chloro-1,3,2-dioxaphospholane.

Table 3
Phenolic, aliphatic, and carboxylic hydroxyl groups present on the examined MWL and LBP at different liquefaction times, determined by quantitative ^{31}P NMR

Functional group (mmol/g)	*Time* 0 min *Sample* MWL	5 min LBP-5	15 min LBP-15	120 min LBP-120	180 min LBP-180	240 min LBP-240
Aliphatic OH	7.44	2.75	2.44	2.09	2.51	2.61
S-OH/P−OH	0.34	0.07	0.06	0.08	0.08	0.09
Phenolic OH	1.11	4.94	5.11	5.30	5.28	5.37
Aliphatic OH/Phenolic OH	6.70	0.57	0.48	0.39	0.48	0.49
(G + H)*	0.82	2.10	2.09	2.03	2.04	2.10
Sr**	0.29	2.84	3.02	3.27	3.24	3.27
COOH	0.13	0.00	0.00	0.01	0.01	0.02
Total OH	8.55	7.69	7.55	7.39	7.79	7.98

*Guaiacyl and *p*-hydroxyphenyl phenolic OH; due to the absence of a well-resolved signal of *p*-hydroxyphenyl (H) moieties, the quantification was performed by integrating the region of 140.2-137.4 ppm that correspond to both – *p*-hydroxyphenyl (H) and guaiacyl (G) phenolic OH groups.
** Syringyl phenolic OH.

2.10 mmol/g) implies a much faster cleavage of the β-aryl ethers with syringyl moieties in the acidic system than in those with guaiacyl moieties. There are also the signals corresponding to the OH in the condensed structures in this area. Therefore, the phenolic OH increase may be additionally influenced by the continuous appearance of the condensed segments.

The determined total OH content after 5 min of the liquefaction remained relatively stable during the prolonged reaction time, indicating the absence of undesirable re-condensation reactions, particularly caused by the intensive lignin self-polymerization reactions in the acidic medium (Table 3).[22]

The aliphatic OH/aromatic OH ratio was found to be significantly decreased, suggesting a preferential degradation of aliphatic side chains with respect to aromatic units. Furthermore, the decrease of aliphatic OH/aromatic OH ratio from 6.70 to 0.49 implies a radical change of the sample nature that reflects in the predominance of aromatic OH.

The carboxylic acids showed a clear decrease during the lignin liquefaction that accordingly implies the presence of esterification reactions induced by EG in the presence of PTSA as a catalyst.

Quantitative Analysis ^{13}C NMR. An inverse gated decoupling sequence was used to quantitatively estimate the lignin and lignin structures (LBP) formed during the liquefaction, especially the incorporation of aliphatic chains into the lignin backbone. This reaction was considered to be the cause of the enhanced solubility of liquefied lignin samples.

The overall amount of aliphatic carbons in the LBP samples was evaluated by integrating the signals in the range of 59.5-69.6 ppm. The increase of aliphatic carbon content with respect to liquefaction time (from 3.0 to 3.7 mmol/g) indicates that EG was introduced into the lignin structure (Table 4). Furthermore, the appearance of a number of overlapped signals in aliphatic carbon region in spectra of the LBP in Figure 3 implies the occurrence of interactions between lignin and aliphatic EG moieties. In contrast to the MWL spectrum

Table 4
Comparison of aliphatic carbons, aromatic and methoxy units content (mmol/g) in MWL and LBP at different liquefaction times as determined by quantitative ^{13}C NMR

Time	Sample	Aliphatic carbons (59.5–69.6 ppm)	Aromatic units (101.0–154.8 ppm)	Methoxy units (55.6 ppm)
0 min	MWL	3.00 ± 0.03	3.40 ± 0.03	5.30 ± 0.05
5 min	LBP-5	4.10 ± 0.04	4.10 ± 0.04	4.30 ± 0.04
120 min	LBP-120	3.70 ± 0.04	3.30 ± 0.03	3.10 ± 0.03
240 min	LBP-240	3.70 ± 0.04	3.30 ± 0.03	2.90 ± 0.03

shown in Figure 3, in both LBP spectra there was only a Cγ signal at 62.6 ppm instead of three characteristic arylglycerol-β-aryl ether signals observed in the aliphatic carbon region. From the obtained data it could be assumed that LBP structures are formed by a preferential cleavage of β-aryl ether bonds in lignin followed by an introduction of the aliphatic EG moieties into the lignin backbone.

The amount of aromatic units was determined by integrating the signals between 101.0 to 154.8 ppm. The initial increase of the aromatic unit content may be interpreted in terms of the lignin degradation, which enables the formation of the low-molecular mass fragments with larger amount of aromatic units (4.1 mmol/g; Table 4). However, the introduction of EG moieties inside the lignin structure affected its overall composition, lowering the relative amount of aromatic units to 3.3 mmol/g during the prolonged lignin liquefaction.

The methoxy group content evaluated by the integration of the signal at 55.6 ppm was determined to decrease from 5.3 to 2.9 mmol/g over the 4 h treatment (Figure 3, Table 4). The decrease in intensity of the signal corresponding to the methoxy groups in LBP is more

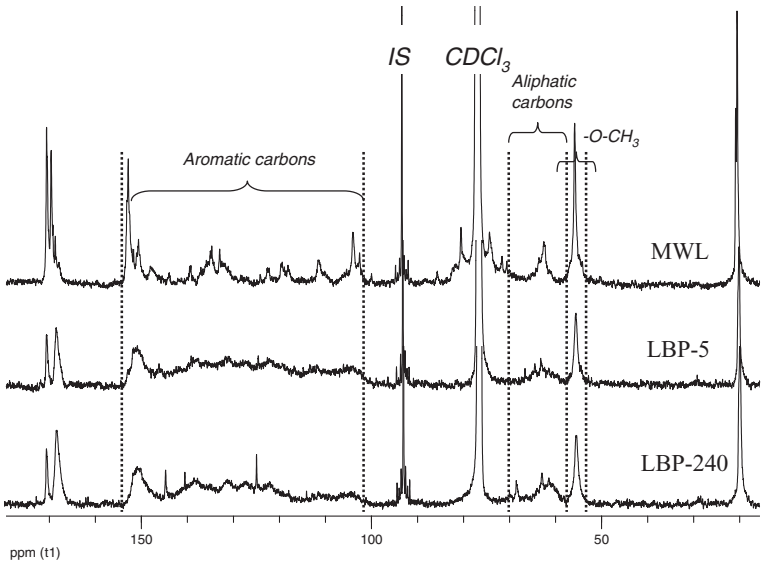

Figure 3. Quantitative ^{13}C NMR spectra of acetylated beech MWL, LBP-5, and LBP-240.

pronounced than the decrease of the aromatic units. This implies, besides an overall severe modification of the lignin structure, the occurrence of demethoxylation and demethylation reactions of guaiacyl and syringyl units within the lignin macromolecule and simultaneous formation of LBP during the liquefaction.

SEC Analysis

In several investigations it has been emphasized that during SEC measurements of polymers in general,[23] and especially of lignins, there occur interactions between lignin molecules (association), lignin and solvent (solvatation), and lignin column packing material (adsorption), which all should be minimized in order to obtain absolute molecular mass distributions (MMDs).[24–27] However, it should be emphasized that in many practical applications, as well as in our case, the knowledge of relative molar masses gives important information about changes in the size of lignin molecules during different processes and reactions.

The effects of the liquefaction on the lignin structure were elucidated, evaluating changes in the MMD of the isolated LBP and lignin-glycol samples (LGS) using size-exclusion chromatography (SEC). Due to the polarity and the state differences of the prepared liquid LGS and freeze-dried LBP samples, the SEC analyses were carried out using two different chromatographic systems, as reported in the experimental section. It should be noted that the use of the UV detector, set to 280 nm, suppressed the detection of EG in the LGS samples. For this reason, the chromatograms shown in Figure 4 indicate the presence of structures bearing ketone, aliphatic, and aromatic aldehyde moieties.

The acetylated MWL sample with an average molecular mass ($\overline{M_w}$) of 5800 g/mol was used as a reference material for the obtained LBP samples. The decrease of $\overline{M_w}$ observed during the first 5 min of the liquefaction indicates the initial MWL degradation (Table 5). The increased aromatic region absorbance at 280 nm and the shift of the main peak towards the lower molecular mass of LBP-5 in the chromatogram (Figure 4) confirms the formation of lower-mass MWL fragments.

In contrast to the LBP-5, the increase of $\overline{M_n}$ from 1440 g/mol to 1550 g/mol and greatly reduced aromatic region absorbance at 280 nm of the LBP-15 chromatogram indicate the formation of larger structures followed by the aliphatic EG chain being incorporated into the LBP backbone. Furthermore, the decrease of the overall aliphatic OH content, especially the decrease of *S-OH/P-OH* ratio as determined by the quantitative ^{31}P NMR, implies the occurrence of the condensation reactions between highly reactive secondary aliphatic OH in the lignin macromolecule and an excess of aliphatic OH provided by EG. In addition

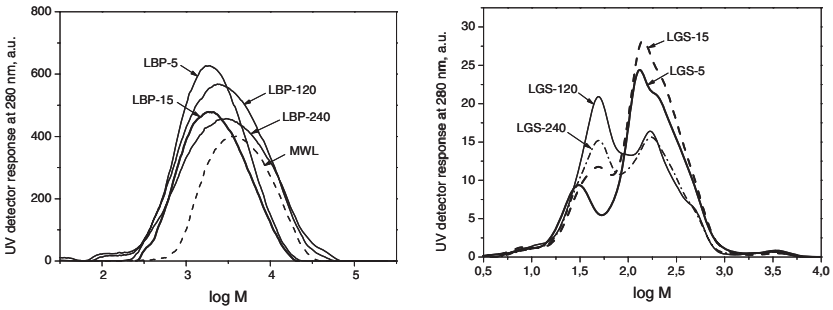

Figure 4. SEC chromatograms of MWL (used as a reference), LBP-5, LBP-15, LBP-120, and LBP-240 samples (left); LGS-5, LGS-15, LGS-120, and LGS-240 samples (right).

Table 5
Weight-average molecular mass ($\overline{M_w}$), number-average molecular mass ($\overline{M_n}$), and polydispersity index (PDI) of MWL (use as reference), LBP, and LGS samples with time of liquefaction

Time	Sample	$\overline{M_w}$, g/mol	$\overline{M_n}$, g/mol	PDI	Sample	$\overline{M_w}$, g/mol	$\overline{M_n}$, g/mol	PDI
0 min	MWL	5800	2990	1.9	—	—	—	—
5 min	LBP-5	2950	1440	2.0	LGS-5	250	70	3.5
15 min	LBP-15	3000	1550	2.0	LGS-15	220	75	3.0
120 min	LBP-120	4700	1390	3.4	LGS-120	210	65	3.3
240 min	LBP-240	5500	690	8.0	LGS-240	190	60	3.2

to the incorporation of aliphatic moieties, the reduction in LBP-15's main peak intensity could be interpreted as a synchronous lignin degradation and a formation of low-molecular mass fragments that accordingly increased the aromatic region absorbance at 280 nm of the LGS-15 chromatogram (Figure 4).

After 15 min of the liquefaction, the continuous growth of $\overline{M_w}$ and the decrease of overall aliphatic OH content determined by quantitative ^{31}P NMR imply the presence of condensation reactions, presumably involving less reactive primary aliphatic OH groups at the C γ position in the lignin phenyl propane units and/or obtained after EG incorporation (Figure 4). In addition to the formation of large LBP structures that can be deduced from the shift of the main peak to the higher molecular mass (Figure 4; LBP-120), the increased aromatic region absorbance at 280 nm followed by an enlarged PDI and reduced $\overline{M_n}$ indicate the occurrence of lower molecular mass fragments enriched with aromatic moieties. The observed extensive reduction of the LGS-120's main peak intensity may explain the formation of fragments with increased $\overline{M_w}$, caused by condensation between non-etherified syringyl and guaiacyl units and EG. Therefore, such structures with a higher amount of aromatic moieties are consequently converted into LBP-120 constituents. Additionally, the extensive reduction of the LGS-120 main peak intensity (Figure 4) might be a result of a simultaneous degradation of the lignin-derived compounds deduced from the appearance of an intense peak at the lower molecular mass region.

During the next 120 min of lignin liquefaction, the $\overline{M_w}$ of LBP-240 increased to 5500 g/mol. However, the simultaneously reduced $\overline{M_n}$ implies that the degradation and condensation processes occurred concurrently. Due to the invariability of the aliphatic carbon content after 120 min of treatment, as determined by quantitative ^{13}C NMR analysis, it can be assumed that LBP-240 high-molecular mass fraction is formed by inter-condensation between the present LBP fragments without the additional aliphatic chain incorporation that is demonstrated by the reduced aromatic region absorbance at 280 nm (Figure 4). Furthermore, the gradually increasing content of aliphatic OH, which occurred until the end of the reaction as determined by the ^{31}P NMR as well as the enlarged PDI to 8.0 (Table 5), indicates the occurrence of lower-molecular mass LBP fragments that could be the result of both a simultaneous degradation of the newly formed LBP macromolecules and the formation of larger lignin-derived structures in the LGS-240, followed by the synchronous conversion into LBP-240 constituents. The latter can be confirmed by the reduced intensity of the peak at lower-molecular mass region (Figure 4; LGS-240). Furthermore, the increase of LBP-240 polydispersity with the reaction time could be interpreted as additional condensation

reactions between LBP segments obtained after LBP macromolecule degradation with EG and low-molecular mass lignin-derived products.

The occurrence of condensation reactions between low-molecular mass lignin-derived compounds in LGS and EG during the first 15 min of the treatment could be deduced from the initial increase of $\overline{M_n}$ and the synchronous PDI value decrease as listed in Table 5. Thus, the formed LGS fragments with increased $\overline{M_w}$ were converted into LBP constituents and simultaneously eliminated from LGS. Furthermore, the continuous low-molar mass compound condensation with EG followed by synchronous elimination of larger fragments from LGS with time is confirmed by the slow $\overline{M_w}$ and $\overline{M_n}$ decrease from 220 g/mol and 75 g/mol to 190 g/mol and 60 g/mol, respectively (Table 5).

The results obtained by the two analytical techniques, size-exclusion chromatography and quantitative NMR analysis, suggest a presence of a few parallel chemical reactions during the lignin liquefaction. Evidently, gradual EG incorporation into the lignin backbone formed a condensed LBP material with predominant aromatic hydroxyl groups.

LBP Formation by DEPT Analysis

The qualitative DEPT analysis was used to follow the MWL reaction with EG during the liquefaction reaction, where MWL was used as a reference. The newly appeared signals in the aliphatic carbon region (Figure 5) indicate the occurrence of a number of parallel EG and lignin interactions. According to the previously discussed quantitative NMR and SEC data, the high number of overlapped peaks in the aliphatic carbon region at the beginning of the reaction confirms that the initial MWL degradation is followed by the incorporation of EG chains into the lignin macromolecule.

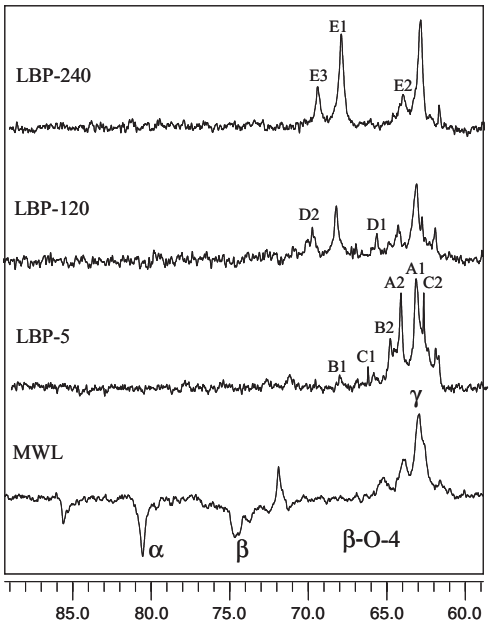

Figure 5. DEPT spectra of beech MWL and of samples taken after 5 min, 120 min, and 240 min of beech MWL liquefaction.

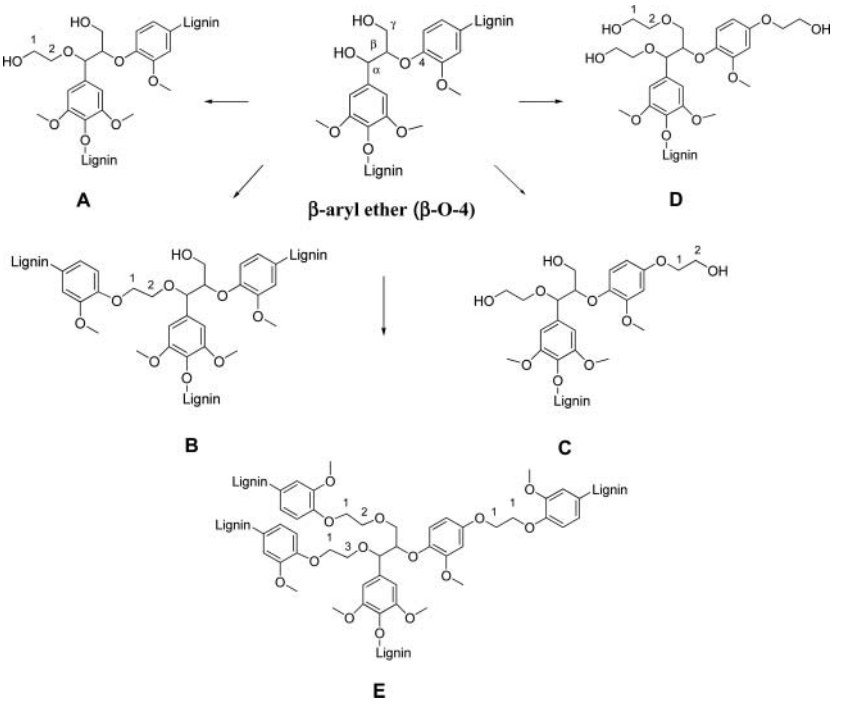

Figure 6. Tentative sub-units formed during MWL reaction with EG.

An attempt to compose the structures that could show an eventual EG chain incorporation into the lignin backbone was made. The newly emergent peaks in the aliphatic carbon region were designated according to the literature.[23–25] The quantitatively most important inter-unit linkage in lignin, the β-O-4 linkage depicted in Figure 6, was used to present the potential EG incorporation pathway into the lignin macromolecule. A number of additional peaks in LBP-5 spectrum indicate the presence of a few simultaneous reactions. A tentative assignment of **A1, A2, B1, B2, C1** and **C2** signals in Figure 5 and previously discussed quantitative ^{31}P NMR data enabled us to determine that initially formed sub-units were a result of an EG attack at the Cα position of the phenyl propane segments (**A**), followed by the synchronous condensation between aromatic lignin constituents and incorporated EG chains (**B, C**). The assignation of **D1** and **D2** signals that occurred after 120 min of the treatment indicates an EG reaction with less reactive primary lignin hydroxyl groups and consequently forming **D** segments. Finally, well-defined and intensive signals (**E1, E2, E3**) corresponding to the $-Ph-O-CH_2-CH_2-O-Ph-$ fragments in the LBP-240 spectrum imply the predominance of **E** segments. Thus, the gradual EG introduction into the lignin backbone and accordingly increasing molar mass during the liquefaction reaction confirms the formation of condensed lignin-based polymeric material (LBP).

Identification of Lignin Degradation Products in LGS

Lignin-glycol samples (LGS) were subjected to HPLC analysis in order to identify the low-molecular mass lignin-derived products obtained after lignin liquefaction in EG with PTSA as a catalyst. These samples were obtained as described in the experimental section.

The qualitative analysis of LGS was performed using the retention times of standards received from Aldrich. Identified products and their retention times (RT) are listed in

Table 6
Lignin-derived products obtained after liquefaction in LGS sample identified by HPLC

Compound	Retention time, min
4-hydroxy-benzoic acid	8.48
4-hydroxy-3-methoxy-benzoic acid (vanillic acid)	10.05
4-hydroxy-3,5-dimethoxy-benzoic acid (syringic acid)	11.37
4-hydroxy-3-methoxy-benzaldehyde (vanillin)	12.54
4-hydroxy-3-methoxy-cinnamyl alcohol (coniferyl alcohol)	13.93
4-hydroxy-3,5-dimethoxy-benzaldehyde (syringaldehyde)	14.05
4-hydroxy-3,5-dimethoxy-cinnamyl alcohol (sinapyl alcohol)	15.71
3,5-dimethoxyphenol	20.90
4-hydroxy-3-methoxy-cinnamic acid (ferulic acid)	23.70

Table 6. The detection of the two most important monolignols–coniferyl and synapyl alcohols–as well as vanillin, vanillic acid, syringaldehyde, and syringic acid–indicates a fast initial lignin degradation. The presence of both aldehyde and carboxylic acid implies the occurrence of simultaneous oxidation and hydrolysis. Ferulic acid in the LGS sample indicates a rapid scission of unsaturated bonds in the coniferyl alcohol and the occurrence of simultaneous coniferyl alcohol oxidation and hydrolysis. The detection of 3,5-dimethoxyphenol and *p*-hydroxy benzoic acid accordingly confirms the presence syringyl and guaiacyl unit demethoxylation reactions, which is in agreement with the data obtained by quantitative ^{13}C NMR analysis.

The use of standard materials enabled us to recognize the majority of products obtained after 5 min of the lignin liquefaction, while at the end of the reaction from all the present products only syringic acid was identified. Since the recognition of the majority of the obtained products was hindered due to the elution at slightly longer RT compared to the ones of external standards, the assumption could be made that the compounds identified at the beginning of the reaction are further modified, presumably by reaction with EG and by an interaction between the formed intermediates.

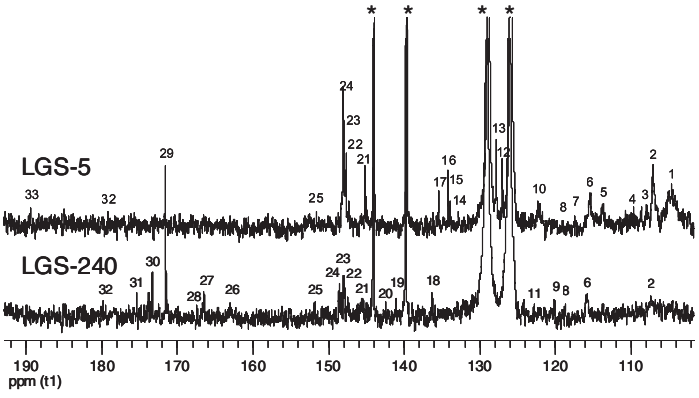

Figure 7. Qualitative ^{13}C NMR spectra of LGS-5 and LGS-240 (aromatic carbon reagion); signals indicated with an asterisk (*) correspond to PTSA.

Table 7
Assignments of ^{13}C NMR signals in region from 102.0 to 193.0 ppm for LGS-5 and LGS-240 samples; solvent: DMSO-d_6

Signal number	Chemical shift, ppm	Assignment
1	104.7	C-2/C-6 in syringyl units
2	107.4	C-2/C-6 in syringic acid
3	108.2	C-2/C-6 in 3,5-dimethoxyphenol
4	111.1	C-2 in guaiacyl units
5	114.1	C-5 in guaiacyl units
6	115.8	C-3/C-5 in *p*-hydroxy benzoic acid
7	117.7	C-5 in vanillin
8	118.7	C-6 in guaiacyl units
9	120.1	C-6 in guaiacyl units, in 5-5′ type
10	122.4	C-1 in *p*-hydroxy benzoic acid
11	122.8	C-6 in ferulic acid
12	127.3	C-1 in ferulic acid
13	128.1	C-β in coniferyl and sinapyl alcohol
14	133.1	C-1 in nonetherified guaiacyl units
15	134.2	C-1 in etherified syringyl units
16	134.4	C-1 in etherified guaiacyl units
17	135.7	C-1 in nonetherified syringyl units
18	136.3	C-1 in nonetherified syringyl units
19	141.1	C-4 in syringic acid ester
20	142.4	C-4 in syringic acid
21	145.4	C-4 in etherified guaiacyl units
22	147.6	C-4 in etherified guaiacyl units; C-3/C-5 in nonetherified syrigyl units
23	147.9	C-4 in nonetherified guaiacyl units
24	148.3	C-3 in nonetherified guaiacyl units
25	151.8	C-3/C-5 in etherified syrigyl units
26	163.1	C-γ in ferulic acid ester
27	166.5	C=O in aromatic ester or acid
28	167.3	C=O in aromatic ester or acid
29	171.6	C-γ in ferulic acid
30	173.3	C=O in aliphatic ester
31	175.5	C=O in aliphatic carboxylic acid
32	179.5	C=O in dienone or quinone units
33	189.5	C=O in aromatic aldehyde

Structural changes of low-molecular mass lignin-derived products in LGS samples were elucidated by qualitative 13C NMR analysis. Principal differences between the LGS spectra at the beginning and at the end of the treatment were observed in the aromatic carbon region. The signals in the aromatic carbon region (102.0 to 193.0 ppm) in LGS-5 and LGS-240 spectra shown in Figure 7 were designated according to the literature[28–30] and summarized in Table 7.

The comparison of the LGS-5 and LGS-240 spectra revealed a significant decrease of signals (22, 23, 24) corresponding to the non-etherified syringyl and guaiacyl substructures

and the appearance of peaks (30, 31, 27, 28) characteristic to the carbonyl (C = O) groups in aliphatic, aromatic esters and acids. In addition, the overall reduction of signal intensity in aromatic carbon region may be attributed to the formation of larger lignin-EG structures with reduced solubility in water followed by their elimination from LGS with time as was determined by SEC. Thus, the larger LGS fragments, which had an increased molar mass, are simultaneously converted into LBP constituents, leaving only low-molecular mass lignin-derived subunits in LGS-240. This is confirmed with the newly appeared signals (30, 31, 27, 28) corresponding to the carbonyl groups and signals (18, 19, 20) characteristic of the non-etherified syringic acid and syringic acid ester. From the obtained results the assumption could be made that lignin degradation products are further modified mainly by esterification and etherification with EG.

Conclusions

Beech milled-wood lignin was used as a model compound to elucidate lignin structural changes during the liquefaction in ethylene glycol under catalysis of sulphuric acid or *p*-toluene sulfonic acid monohydrate. It was determined that the intensity of the lignin condensation reactions depends on hydronium ion concentration. The completely solubilized lignin during the *p*-toluene sulfonic acid monohydrate-catalyzed liquefaction suffered a degradation at the beginning of the reaction, while during the prolonged treatment the condensation reactions with ethylene glycol induced formation of the "lignin-based polymer." Incorporation of ethylene glycol molecule at the Cα position of the phenyl propane segment was confirmed by quantitative ^{31}P NMR analysis. Nevertheless, beside the reduced primary/secondary hydroxyl group ratio, argumentative of primary hydroxyl group substitution, gradual ethylene glycol incorporation into the lignin backbone formed a condensed lignin-based polymeric material with predominant aromatic hydroxyl groups. Furthermore, the quantitative ^{13}C NMR analysis revealed the gradual introduction of ethylene glycol moieties inside the lignin structure that consequently affected its overall composition by lowering the relative amount of aromatic units.

The final lignin liquefaction product composed from high-molecular mass and low-molecular mass fraction was formed during the concurrent degradation and condensation reactions between the lignin degradation fragments and ethylene glycol.

High-performance liquid chromatography enabled the identification of 4-hydroxy benzoic acid, vanillic acid, syringic acid, vanillin, coniferyl alcohol, syringaldehyde, sinapyl alcohol, 3,5-dimethoxyphenol, and ferulic acid in the lignin-glycol sample at the beginning of the lignin liquefaction. Furthermore, the conversion of the initially identified products into the aliphatic, aromatic (syringyl- and guaiacyl-based) esters and acids with the treatment time due to the reaction with ethylene glycol was confirmed by qualitative ^{13}C NMR.

References

1. Lin, L.; Yoshioka, M.; Yao, Y.; Shiraishi, N. Liquefaction of wood in the presence of phenol using phosphoric acid as a catalyst. J. Appl. Polym. Sci. **1994**, *52*, 1629–1636.
2. Lin, L.; Yoshioka, M.; Yao, Y.; Shiraishi, N. Preparation and properties of phenolated wood/phenol/formaldehyde condensed resin. J. Appl. Polym. Sci. **1995**, *58*, 1297–1304.
3. Alma, M.H.; Maldas, D.; Shiraishi, N. Liquefaction of several biomass wastes into phenol in the presence of various alkalis and metallic salts as catalysts. J. Polym. Eng. **1998**, *18*, 162–177.
4. Kobayashi, M.; Asano, T.; Kajiyama, M.; Tomita, B.J. Analysis on residue formation during wood liquefaction with polyhydric alcohol. J. Wood Sci. **2004**, *50*, 407–414.

5. Kurimoto, Y.; Doi, S.; Tamura, Y. Species effects on wood-liquefaction in polyhydric alcohols. Holzforschung **1999**, *53*, 617–622.
6. Kržan, A.; Kunaver, M.; Tišler, V. Wood liquefaction using dibasic organic acids and glycols. Acta Chim. Slov. **2005**, *52*, 253–258.
7. Kunaver, M.; Jasiukaitytė, E.; Čuk, N. Ultrasonically assisted liquefaction of lignocellulosic materials. Bioresour. Technol. **2012**, *103*, 360–366.
8. Yao, Y.; Yoshioko, M.; Shiraishi, N. Water-absorbing polyurethane foam from liquefied starch. J. Appl. Polym. Sci. **1996**, *60*, 1939–1949.
9. Lee, S.H.; Teramoto, Y.; Shiraishi, N. Biodegradable polyurethane foam from liquefied waste paper and its thermal stability, biodegradability, and genotoxicity. J. Appl. Polym. Sci. **2002**, *83*, 1482–1489.
10. Kunaver, M.; Jasiukaitytė, E.; Čuk, N.; Guthrie, J.T. Liquefaction of wood, synthesis and characterization of liquefied wood polyester derivatives. J. Appl. Polym. Sci. **2010**, *115*, 1265–1271.
11. Yamada, T.; Ono, H. Characterization of the products resulting from ethylene glycol liquefaction of cellulose. J. Wood Sci. **2001**, *47*, 458–464.
12. Lin, L.; Yao, M.; Yoshioka, M.; Shiraishi, N. Liquefaction mechanism of cellulose in the presence of phenol under acid catalysis. Carbohydr. Polym. **2004**, *57*, 123–129.
13. Lin, L.; Nakagame, S.; Yao, Y.; Yoshioka, M.; Shiraishi, N. Liquefaction mechanism β-O-4 lignin model compound in the presence of phenol under acid catalysis, Part 2. Reaction behaviour and pathways. Holzforschung **2001**, *55*, 625–630.
14. Lin, L.; Yao, Y.; Shiraishi, N. Liquefaction mechanism β-O-4 lignin model compound in the presence of phenol under acid catalysis, Part 1. Identification of the reaction products. Holzforschung **2001**, *55*, 617–624.
15. Jasiukaitytė, E.; Kunaver, M.; Crestini, C. Lignin behaviour during wood liquefaction–Characterization by quantitative ^{31}P, ^{13}C NMR and size-exclusion chromatography. Catal. Today **2010**, *156*, 23–30.
16. Björkman, A. Studies on finely divided wood. Part 1. Extraction of lignin with neutral solvents. Svensk Papperstidn. **1956**, *59*, 477–485.
17. Guerra, A.; Filpponen, I.; Lucia, L.A.; Argyropoulos, D.S. Comparative evaluation of tree lignin isolation protocols for various wood species. J. Agric. Food Chem. **2006**, *54*, 9696–9705.
18. Guerra, A.; Filpponen, I.; Lucia, L.A.; Saquing, C.; Baumberger, S.; Argyropoulos, D.S. Towards a better understanding of the lignin isolation process from wood. J. Agric. Food Chem. **2006**, *54*, 5939–5947.
19. Argyropoulos, D.S.; Bolker, H.I.; Heither, C.; Archipov, Y. 31P NMR spectroscopy in wood chemistry part V. Qualitative analysis of lignin functional groups. J. Wood Chem. Technnol. **1993**, *13*(2), 187–212.
20. Argyropoulos, D.S. Quantitative phosphorous-31 NMR analysis of lignins, a new tool for the lignin chemist. J. Wood Chem. Technol. **1994**, *14*, 45–63.
21. Granata, A.; Argyropoulos, D.S. 2-Chloro-4,4,5,5-tetramethyl-1,3,2-dioxaphospholane, a reagent for the accurate determination of the uncondensed and condensed phenolic moieties in lignins. J. Agric. Food Chem. **1995**, *43*, 1538–1544.
22. Lai, Y.Z., Sarkanen, K.V. *Lignin Occurrence, Formation, Structure and Reactions*; Wiley-Interscience: New York, 1971, 165–240.
23. Yau, W.; Kirkland, D.; Bly, D. *Modern Size-Exclusion Liquid Chromatography*; John Wiley & Sons: New York, 1979.
24. Himmel, M.E.; Mylnar, J.; Sarkanen, S. Size exclusion chromatography of lignin derivatives. In *Handbook of Size Exclusion Chromatography*; Wu, Chi-san, Ed.; Chromatographic Science Series 69; Marcel Dekker, Inc.: New York, 1995, 353–379.
25. Pla, L. Light scattering and vapour pressure osmometry. Determination of molecular weight, size and distribution. In *Methods in Lignin Chemistry*; Lin, S.; Dence, C., Eds.; Springer-Verlag, Berlin, 1992, 498–517.
26. Sjöström, E.; Alen, R. In *Analytical Methods in Wood Chemistry, Pulping and Papermaking, Springer Series in Wood Science*; Timell, T.E., Eds.; Springer Verlag: Berlin, 1999.

27. Glasser, W.G.; Vipul; Frazier, C.E. Molecular weight distribution of (semi-) commercial lignin derivatives. J. Wood Chem. Technol. **1993**, *13*(4), 545–559.
28. Kishimoto, T.; Ueki, A.; Sano, Y. Delignification mechanism during high-boiling solvent pulping. Part 3. Structural changes in lignin analyzed by ^{13}C-NMR spectroscopy. Holzforschung **2003**, *57*, 602–610.
29. Sun, X.F.; Sun, R.C.; Fowler, P.; Baird, M.S. Extraction and characterization of original lignin and hemicelluloses from wheat straw. J. Agric. Food Chem. **2005**, *53*, 860–870.
30. Capanema, E.A.; Balakshin, M.Y.; Kadla, J.F. Quantitative characterization of a hardwood milled wood lignin by nuclear magnetic resonance spectroscopy. J. Agric. Food Chem. **2005**, *53*, 9639–9649.